Acta Cryst. (1997). B53, 620–630

Cleavage and Twinning in $CuInSe_2$ Crystals

Z. A. SHUKRI AND C. H. CHAMPNESS*

Electrical Engineering Department, McGill University, 3480 University Street, Montreal, Quebec, Canada H3A 2A7. E-mail: champnes@ee.lan.mcgill.ca

(Received 13 March 1997; accepted 20 March 1997)

Abstract

A study was made of the cleavage and twinning character in single crystals of the chalcopyrite $CuInSe_2$, copper indium diselenide, grown in the laboratory by a vertical Bridgman method. In this material, with a *c/a* ratio of 2.006, the two main cleavage orientations were found to be {101} and {112} (corresponding to the descriptions {201} and {111}, respectively, in a cubic lattice). The plane identifications were made by measuring angles between adjacent cleaved surfaces and verifying the orientations by X-ray Laue and diffractometry. Cleavage was also found less frequently in a {110} plane, but here microscopic examination of the surface revealed it to consist of ridges in a <110> direction, where the microplanes on either side of a ridge edge were {112} planes. Twinning in the grown crystals was found, by angle measurements and X-ray diffraction, to occur along {112} planes, which is similar to the result in face-centred cubic, diamond and zinc blende lattices, where they are the corresponding {111} planes.

1. Introduction

The chalcopyrite $CuInSe_2$ is an important candidate material for thin-film solar cells on account of its high optical absorption coefficient and chemical stability. While thin films of the compound for this application are likely to be polycrystalline, due to the economics of device fabrication, there is evidence of improved performance with the preferred orientation of the grains. Because of this and a need for determination of its fundamental properties, plus the easier handling of bulk material for etching, polishing and annealing studies, single crystals of $CuInSe_2$ have been grown in this laboratory, employing a one-ampoule vertical Bridgman method. Using suitable techniques (Shukri, Champness & Shih, 1993; Yip, Shih & Champness, 1993) the resulting crystals are found to be void-free, microcrack-free and uniform in composition and conductivity type *n* or *p*. The present paper is an experimental investigation of the cleavage character of these crystals, all of which were *p*-type, prepared from stoichiometric starting proportions of the elements copper, indium and selenium in high-purity form.

In earlier work by Massopust, Ireland, Kazmerski & Bachmann (1984) it was reported that $CuInSe_2$ single crystals could be easily cleaved along {110} planes, but it is possible that this was a mistake in plane description for a chalcopyrite lattice (with a *c/a* ratio close to 2) and {101} was meant instead, as already reported for the chalcopyrite mineral $CuFeS_2$ by Wolff & Broder (1959). More recent results for $CuInSe_2$ by Yip, Weng, Li, Shih & Champness (1991) indicated cleavage along

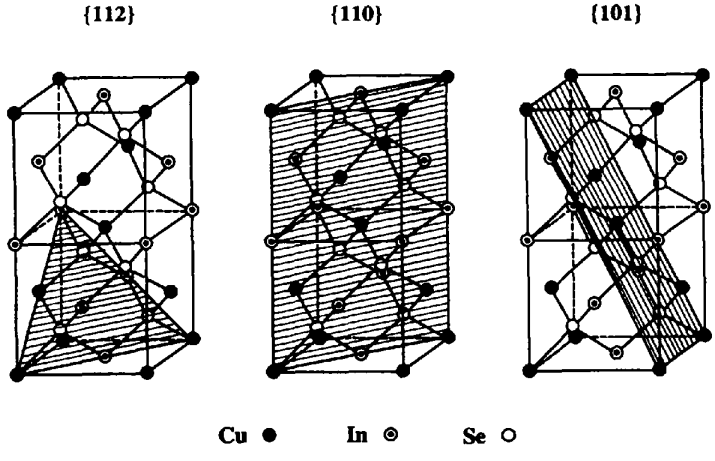

Fig. 1. Chalcopyrite unit-cell schematic diagrams, indicating the three principal cleavage planes: {112}, {110} and {101}.

{112}, {101} and {110} planes, corresponding to {111}, {201} and {110} planes, respectively, in a cubic crystal. However, up until now a detailed intensive study of all the prominent cleavage planes in $CuInSe_2$ has not been made. The present paper is therefore a description of a comprehensive investigation to supply this need. The work consisted of angle measurements between cleaved surfaces and their identification by X-ray diffraction. The plane of twinning was also identified in the bulk monocrystals.

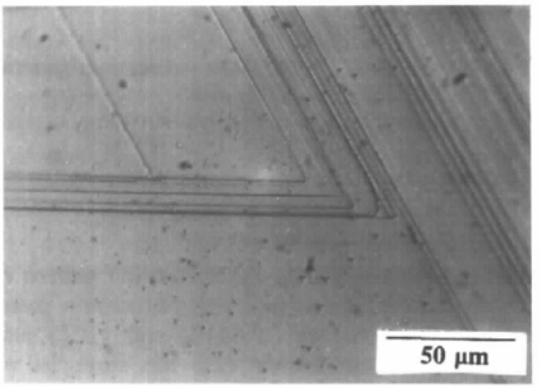

(*a*)

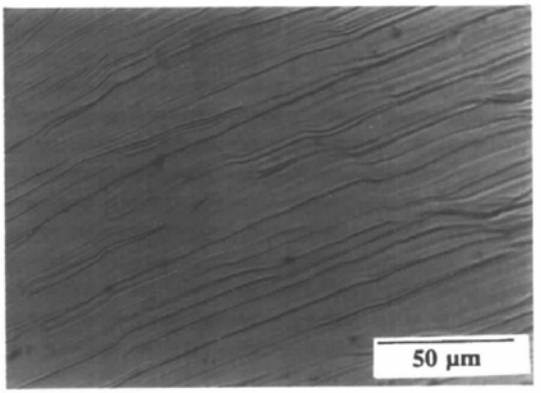

(*b*)

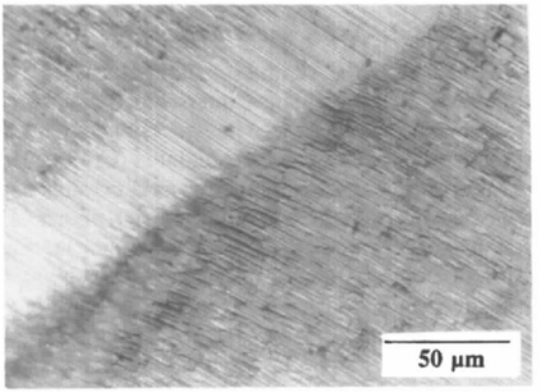

(*c*)

Fig. 2. Photomicrographs of cleavage planes in $CuInSe_2$ crystals revealing surface features of the planes (*a*) {112}, (*b*) {101} and (*c*) {110}.

2. Cleavage planes

Single crystal samples of $CuInSe_2$ were cleaved by applying gentle pressure at room temperature on opposite ends of a grown ingot, without a particular orientation, using a sharp cutting blade. While this technique was rather simple, it was possible to obtain cleavage planes ranging from 5 to 100 mm^2 in area. In some of the samples the applied pressure resulted in a conchoidal, almost glass-like, fracture which was not helpful for the purpose of this study. Frequently, however, the single crystal ingot cleaved into two pieces, each revealing a macroscopically flat plane.

While many cleaved samples were obtained, only three distinct cleavage planes were identified in the $CuInSe_2$ crystals, namely the {112}, {101} and {110} planes. These planes are shown schematically in the chalcopyrite unit cell, as shaded areas, in Fig. 1. The chalcopyrite description of the planes assumes a unit cell with a *c/a* ratio of 2, which is very close to the actual value of 2.006 reported by Shahidi, Shih, Araki & Champness (1985). A photograph showing a perpendicular view for each of the three cleavage planes on actual samples is given in Fig. 2, as observed under an optical microscope. In Fig. 2(*a*) it is seen that the cleavage in the {112} plane is essentially flat, but exhibits terraces with edges that define angles of 60 or 120° between them. These characteristics are typical of the threefold symmetry of this plane. The {101} plane, shown in Fig. 2(*b*), also exhibits some terracing, but the curved nature of the edges of the terraces on this plane distinguishes it from the {112} and {110} planes. The {110} plane, however, has a completely different appearance, as shown in Fig. 2(*c*). Here, the clearly visible straight and parallel striations represent parallel V-shaped ridges, as revealed by the SEM (scanning electron microscope) photograph in Fig. 3. It is seen here that the planes on either side of a ridge are flat and have a constant angle between them, which was

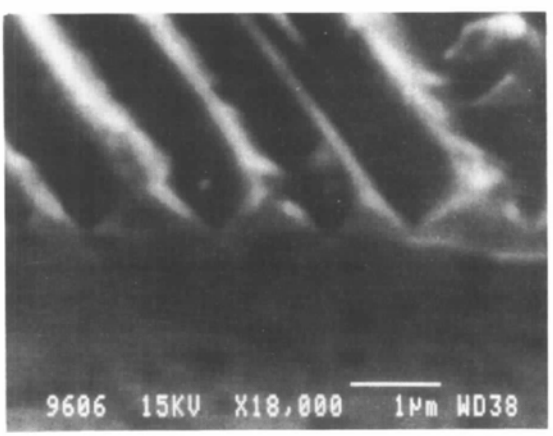

Fig. 3. SEM photograph of the {110} plane, showing the parallel ridges pointing in a <110> direction.

Table 1. *Angle measurements between macroscopic cleavage planes in $CuInSe_2$ crystals*

Only those angles between planes having a common edge are included. The total number of angles (edges) measured was 22. The total number of samples was 11. Accuracy of measurement ±0.1°. Angle calculated assuming the chalcopyrite unit cell has a $c/a = 2$. Measurement of defining planes was carried out to confirm the crystallographic plane provided the cleavage was large enough.

Angle (°)		Defining planes	Plane identification		Angle frequency (number of samples measured with angle)	Comments
Measured	Calculated	{*HKL*}-{*hkl*}	Laue	XRD		
39.4	39.23	{112}-{101}	On both Planes	On both Planes	2	
50.8	50.77	{110}-{101}	{110}	{110}	2	
53.3	53.14	{101}-{101}	Both	Both	2	
70.5	70.53	{112}-{112}	Both	Both	1	
75.0	75.04	{112}-{101}	{112}	Both	3	
78.6	78.46	{101}-{101}	Both	Both	3	
90.1	90.0	{112}-{110}	Both	{110}	2	A 90° angle was not observed between {110} planes
180.1	180.0	{112}-{112}	Both	—	1	Parallel {112} cleavage
180.2	180.0	{101}-{101}	Both	—	1	Parallel {101} cleavage
150.3	None	{101}-{101}	Both	Both	5	Angle between twin crystals

measured, as described in the next section, and found to be about 70°. This indicates that the side planes are {112} microplanes.

Confirmation of the crystallographic orientation of the planes was carried out using X-ray diffractometry, on a Rigaku diffractometer model D/Max-2400 with the $K\alpha$ beam from a copper target. Fig. 4 shows an X-ray diffractogram of a {112} cleaved plane, scanned between 10 and 100° of 2θ, where θ is the Bragg angle. The principal peak, shown at a 2θ value of about 26.51°, corresponds to a lattice d spacing of 3.359 Å, which is in accordance with that from powder diffraction data. Less intense second- and third-order reflections from the parallel {224} and {336} planes are also noted, where the Bragg condition is also satisfied. It is noted here that the weak {224} peak, measured on a single crystal surface, is not observed in the diffraction pattern of a powdered sample of this material. Diffraction patterns were also taken on cleaved {110} and {101} planes (not shown). In the former case the strongest peak corresponded to the {220} plane at $2\theta = 44.18°$, but {110} and {440} peaks were also observed. The third order reflection, from the {330} plane, was not apparent but this is forbidden, at least in the diamond structure. The diffraction pattern from a cleaved {101} plane (not shown) indicated {101}, {303}, {404} and {505} peaks, but no second-order {202} reflection.

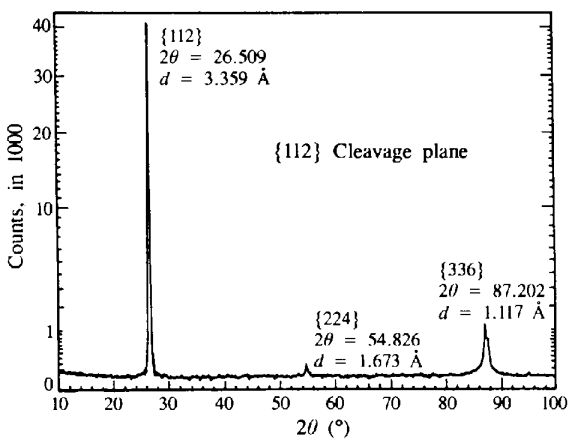

Fig. 4. X-ray diffraction scan of the {112} cleavage surface in $CuInSe_2$, showing an intense peak from the {112} plane and weaker peaks from the {224} and {336} planes. Note that the ordinate is a square-root scale.

Fig. 5 shows characteristic Laue X-ray reflection photographs of the three cleavage planes, along with schematic diagrams of the corresponding spot patterns. Shown also are the axes of symmetry in each case. Here, it is easy to see that the {112} plane has three such symmetry axes, as indicated by the broken lines in Fig. 5(*a*), while the {110} has two axes (Fig. 5*b*) and the {101} only one axis of symmetry (Fig. 5*c*).

3. Angle measurements

The cleaved $CuInSe_2$ samples exhibited angles where two or three cleavage planes intersected. Since in any known crystal structure the angles between any two crystallographic planes can be calculated (Cullity, 1978), a measurement of these angles on actual crystals can be used as a means of identifying the cleavage planes in that crystal system. This assumes, of course, that the angles measured belong to one crystal and also that the method of measurement has sufficient accuracy. Accordingly, on the $CuInSe_2$ crystals grown by the Bridgman method, angles were measured on some 11 separate samples obtained from ingots having some 22 different angles (edges). In order to measure the angles with sufficient accuracy a high-precision goniometer was used for this purpose, with a He–Ne laser, having a beam width of

about 1 mm, as the light source. With this arrangement, an accuracy of *ca* $\pm 0.1^\circ$ in the measured angle was possible. Table 1 gives a summary of all the angles measured on all the crystal samples using this method. In an additional experiment the angle between the two adjacent faces of a microridge on a {11**0**} surface (Fig. 3) was also estimated. The resulting angle of about 35° between the {11**0**} surface and the ridge plane confirms that the ridge faces are indeed {11**2**} planes.

In column 1 of Table 1, the measured angles are shown. As can be seen, only eight unique angles were found from the measurements on the samples with large cleavage planes (excluding the two 180° between parallel cleavages). The measured angles are compared with their calculated values, given in column 2, where it is evident that there is agreement to within $\pm 0.1^\circ$. The crystal planes that define the individual angles are given in column 3 of Table 1. In all but one of the cases the planes defining the angle were identified easily, by comparing the measured angle values with the calculated ones. In the case of the 90.1° angle it was necessary to identify the crystal planes using a Laue photograph as well as X-ray diffractometry (columns 4 and 5). This is because a 90° angle also occurs between two {11**0**} planes or between two {10**1**} planes. This can be seen in Table 2, where all the possible calculated angles, between the three main cleavage planes, are tabulated. In the case of the 150.3° angle (last row of Table 1) no match was found with any calculated crystal angle. A Laue and an X-ray diffraction scan were taken on both planes of this sample and it was revealed that both were {10**1**} planes. While this was puzzling at first, since

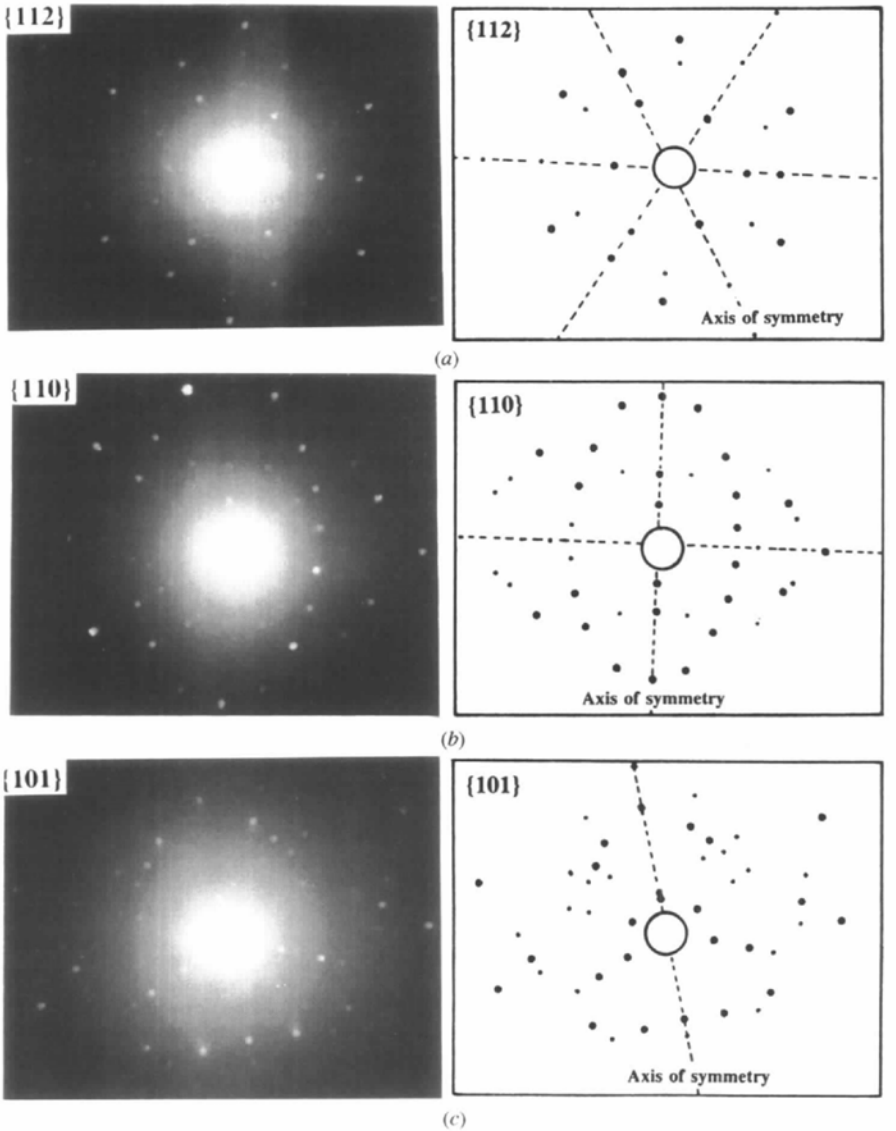

Fig. 5. Characteristic Laue X-ray reflection photographs of the three cleavage planes in $CuInSe_2$, shown with schematic diagrams of the reflected spot patterns for the (*a*) {11**2**}, (*b*) {11**0**} and (*c*) {10**1**} planes. The dashed lines indicate the axes of symmetry in the spot patterns. The smaller spots in the schematics represent faint reflections in the photographs.

Table 2. *Angles between principal cleavage planes in $CuInSe_2$*

Only the {112}, {101} and {110} chalcopyrite crystal planes are listed here. Angles calculated assuming the c/a ratio to be exactly 2 in the chalcopyrite unit cell for $CuInSe_2$.

Cleavage planes {*HKL*}-{*hkl*}	Angles between planes (°) Calculated	Observed
{112}-{112}	70.53	70.5
{112}-{101}	39.23	39.4
	75.04	75.0
{112}-{110}	35.26	35.0*
	90.00	90.1
{101}-{101}	53.13	53.3
	78.46	78.6
{101}-{110}	50.77	50.8
{110}-{110}	90.00	—†

*Observed between the {110} surface and the {112} microcleavage ridges. †A second {110} cleavage was not observed, so that this angle could not be checked.

there is no such angle between two {101} planes in one crystal, it was later found that this angle occurred frequently between {101} planes involving a crystal and its twin. This will be described in more detail in the next section. The frequency of occurrence of all the observed angles is shown in column 6 of Table 1. While the total number of samples measured was not large enough to draw any statistical conclusions, it does appear that some 20% of these measured crystal samples contained twinning, as evidenced by the frequency of occurrence of the 150° angle. It is also evident in these results that occasionally it was necessary to rely on X-ray diffraction to confirm the orientation of the cleavage planes. This, however, should not detract from the usefulness of the measurement of angles for identifying crystal planes, particularly if a large number of samples is involved. Due to the fact that only one {110} cleavage was found, it was not possible to verify the expected 90° angle between two such planes. Further, the angle of 35.26° between a {112} and a {110} plane was not observed for large {112} cleaved planes, but it was observed as 35° between the only {110} cleaved plane and the {112} microplanes of the V-shaped grooves.

Fig. 6 presents a photograph and a schematic of a representative sample exhibiting a well defined angle of 90°. This is the same sample listed in row 7 of Table 1. The planes defining the angle are the {110} and {112} planes indicated on the schematic in Fig. 6(*a*). The {110} plane on the top side is seen to be dark, while the {112} plane on the right-hand side is shiny. This is due to the effect of light on the sample. The angle itself is better seen in Fig. 6(*b*), where a view of the same sample from a perspective parallel to both cleavage planes is shown. Here, the reader may use a protractor to verify the 90° value of the angle. In the next section results specifically on twinning are presented.

4. Twinning

In this section results are specifically reported on the observation of a twinning plane in crystals of $CuInSe_2$. Three single crystal samples with cleavages along the {112}, {110} and {101} planes were studied and found to reveal twinning. The twinning was detected visually by properly orienting the cleaved or polished sample under a collimated light source, revealing shiny and dark regions exhibiting straight edges. Laue photographs were used to examine the orientation of twinned regions in these crystals. From these measurements it was deter-

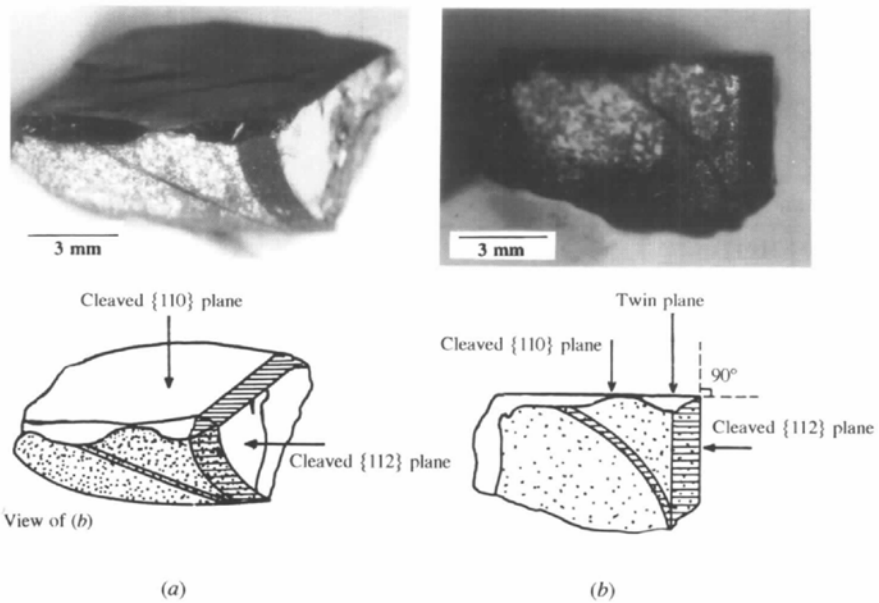

Fig. 6. Photographs and schematics of a representative sample of $CuInSe_2$, exhibiting {110} and {112} cleavage planes with 90° between them. (*a*) A three-dimensional perspective and (*b*) a view parallel to both cleavage planes.

mined that the twinning plane observed in these $CuInSe_2$ samples was in fact a {112} plane. No other twinning plane was found in this study.

In order to reveal the crystallographic orientation of the twinned crystals the X-ray back-reflection Laue method was used for this purpose. Fig. 7 shows a photograph of a crystal with a large {112} cleavage plane. The cleavage plane consists of two regions separated by a ridge, a larger upper region, termed crystal *A*, and a smaller lower region, crystal *B*. The lower portion of the cleavage plane represents a twinned crystal and is shown as the shaded area in the schematic of Fig. 7(*b*), while the upper portion, crystal *A*, is shown unshaded. In the photograph, while the {112} cleavage planes of crystals *A* and *B* appear similar, the exterior surfaces of the crystals show a different reflection of light. Crystal *B* exhibits a shiny narrow band which stretches along the entire ingot exterior parallel to the cleavage plane, while crystal *A* has a darker appearance. This is also shown schematically in Fig. 7(*b*). The orientation of the {112} cleavages of crystals *A* and *B* are different. Two

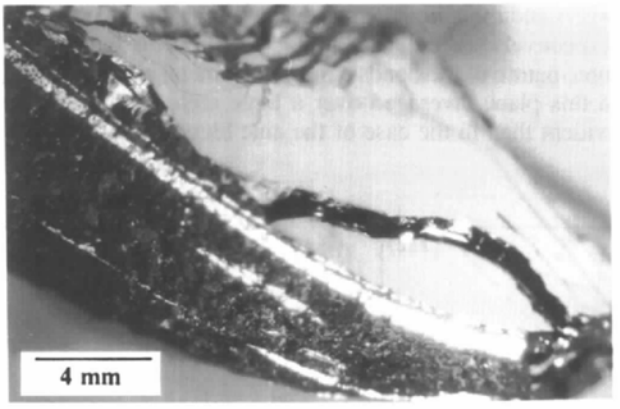

(*a*)

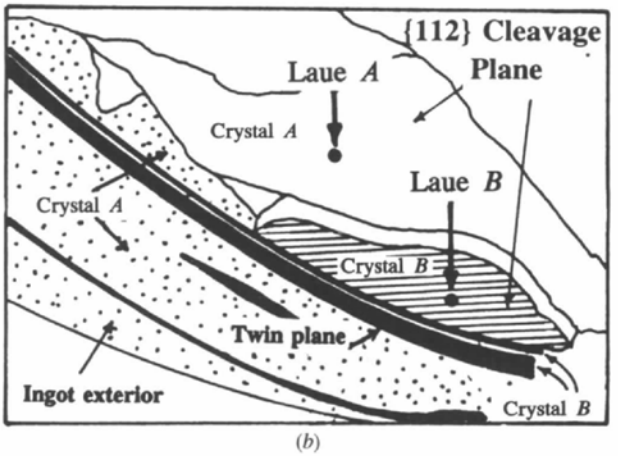

(*b*)

Fig. 7. (*a*) Photograph of a twinned $CuInSe_2$ sample cleaved in the {112} plane. (*b*) Schematic showing the twinned region in this sample and the position of the two Laue pictures of Fig. 8.

Laue photographs were taken on the {112} cleavage, as shown on the schematic, as Laue *A* and Laue *B*. The Laue pictures are shown in Fig. 8 with schematics of the spot patterns. A close examination of the two schematics reveals that the spot pattern of Laue *B* can be generated by a rotation of that of Laue *A* of 180° about an axis normal to the page. This is emphasized by the large arrows on the two schematics. This shows that twinning in this crystal occurs parallel to the {112} plane with rotation about a [221] axis. This fact was also evident in Fig. 6(*b*), shown earlier, where a twin plane indicated on the schematic is also shown to be parallel to a cleaved {112} plane in that sample.

A closer look at the actual interface between two twins is shown by the photomicrograph in Fig. 9, where the sample surface is a (110) plane parallel to the page. The (112) twinning plane is perpendicular to the page and the ridges in each crystal are in <110> directions, creating the same angles of about 55° to the twinning plane.

Fig. 10 shows a sectional view of another twinned sample. The view here shows three adjacent crystal regions, two of which are labelled crystals *A* and *B* in the schematic. The boundary of the twinning {112} plane between crystals *A* and *B* is also quite evident as the oblique straight line, again perpendicular to the plane of the page. The top edge of the sample represents the location of the cleavage planes of the crystals. In this case both crystals *A* and *B* were cleaved along the {101} plane, as indicated by the schematic, perpendicular to the page. As a result of the twinning the cleaved planes make an obtuse angle of about 150° between themselves. This is the same anomalous angle mentioned earlier in Table 1. However, here it is easy to understand how this happens. The twin plane, being a {112} plane, makes an angle of 75.04° with each of the {101} cleavage planes. Therefore, the total angle is twice this, giving a value of 150.08°. Laue photographs were taken on the cleaved {101} planes of both crystals *A* and *B*, as indicated by the arrows in the schematic of Fig. 10(*b*), to reveal their respective orientations. Here, in order for the X-ray beam to be normal to the sample surface in each Laue exposure, the sample had to be rotated by some 30° about an axis (not shown) parallel to the line of intersection of the {101} cleavage planes. The resulting spot patterns are shown in Figs. 11(*a*) and 11(*b*). Again it is seen here that the pattern of Laue *B* can be obtained from that of Laue *A* by a simple rotation about the indicated horizontal axis by 180°, confirming that the two regions are indeed twinned crystals. The angles θ_1 and θ_2 between the rotation axis and the symmetry axis of each pattern are again equal.

Fig. 12 shows a photograph of a ball and stick crystal model of a twin in a $CuInSe_2$ crystal along with its schematic. Here, the horizontal solid line on the schematic in Fig. 13(*b*) indicates where the twinning plane occurs. The dashed arrows in each of the two

crystals are the <110> directions and the angle between either of these directions and the {11**2**} twinning plane is 54.74°. It is seen here that, in going across the twinning plane, from crystal *A* to crystal *B*, the order of the apparent 'long' and 'short' bonds reverses. If the two crystals were separated at the twin plane and one was rotated by 180° about a [221] axis perpendicular to the twinning plane, the twinning would be eliminated. The twin is thus an orthotwin (Holt, 1964) of the rotation type and not a reflection- or para-twin.

5. Discussion

The work in this paper clearly confirms that the principal cleavage planes in $CuInSe_2$ are {11**2**}, {10**1**} and {11**0**}. While the {11**2**} and {10**1**} cleavage surfaces appeared mirror-like and were essentially flat, the physical surface of the {11**0**} plane, by contrast, consisted of V-shaped ridges or grooves, where the planes on each side of the ridge are {11**2**}. The {10**1**} planes showed parallel terracing with edges having no special direction, while the {11**2**} planes, on the other hand, showed less parallel terracing, but with edges exhibiting triangular patterns having 60° angles between them. It is important to point out that these three sets of planes were the *only* cleavage planes found in the Bridgman-grown crystals and that other low-index planes, such as, for example, the {100}, {111} or {221} planes, were not observed. Only one angle was not measured and that was the expected 90° between two {11**0**} planes, because a second {11**0**} cleavage was not observed.

In silicon and germanium, having the diamond structure, the {111} plane is the predominant cleavage plane (Wolff & Broder, 1959; Bean & Gleim, 1969) due to its low density of bonds of $4/(3)^{1/2}$ per $\mathbf{a}^2$, where **a** is the side of the cubic unit cell. By contrast, for III–V compounds, such as GaAs (Wolff & Broder, 1959; Pfister, 1955; Abrahams & Ekstrom, 1960; Ghandi, 1983) and CdTe (Wolff & Broder, 1959; Lorenz, 1962; Iwanaga, Tomizuka & Shoji, 1991), a II–VI compound, all crystallizing in the zinc blende structure, the most common cleavage plane is not the {111}, but the {110} plane [bond density $2(2)^{1/2}$ per $\mathbf{a}^2$]. In these compounds the bonds across the {111} plane are not purely covalent, but also have an ionic character due, in the case of GaAs, for example, to opposite ionic charges on the Ga and the As atoms, thereby giving rise to a coulombic attraction between consecutive {111} planes. This renders cleavage along this plane less likely than in the diamond structures. In the chalcopyrite $CuInSe_2$ the {11**2**} plane layers consist of alternating Se (group VI) layers and metallic layers of Cu and In (groups I and III, respectively), as indicated in Fig. 13(*a*). The extent of the ionic nature of the bonds between the metal and Se layers in this plane, averaged over a large area, could be less evident than in the case of the zinc blende and thus, the

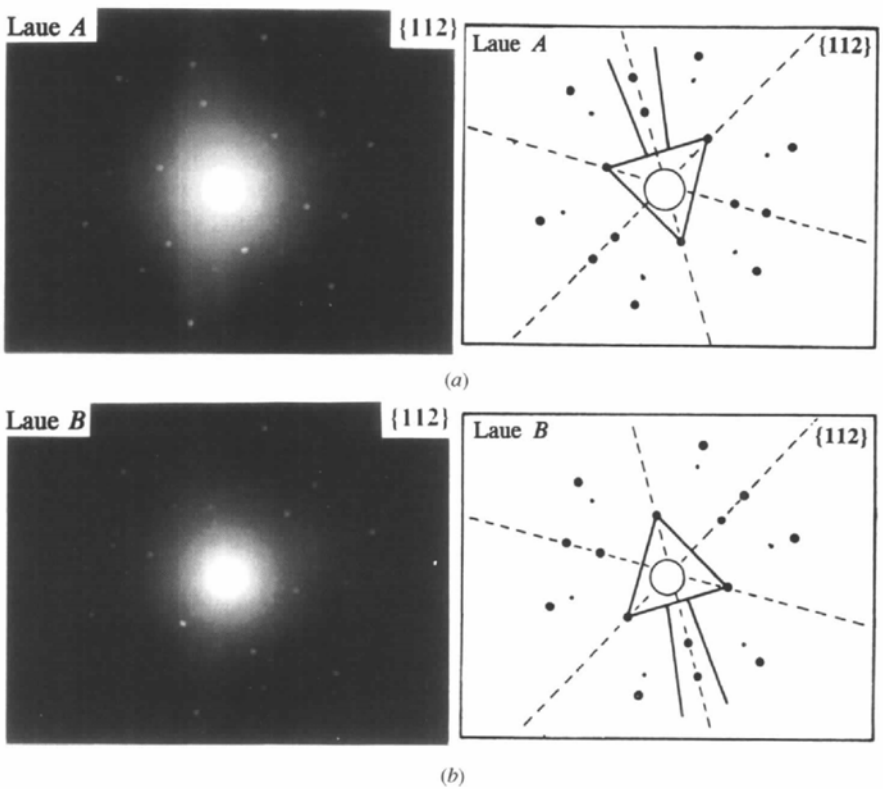

Fig. 8. X-ray Laue photographs on the twinned {11**2**} cleaved sample of Fig. 7. (*a*) Pattern of crystal *A* (Laue *A*); (*b*) pattern of the twinned crystal *B* (Laue *B*). The schematics show coincidence of the spot pattern on rotation by 180° about an axis perpendicular to the page.

{112} cleavage in the chalcopyrite occurs more readily. The opposite may be true, however, for the case of the {110} plane. In this plane for the zinc blende materials there are equal numbers of Ga and As atoms (in GaAs, for example), making this plane on average electrically neutral. In the case of the chalcopyrite lattice, however, the Cu and In atomic positions alternate across this plane (Fig. 13*b*) and hence there would still be some localized coulombic attraction between consecutive {110} planes. As a result, instead of a flat {110} cleavage, such as the *AB* plane in Fig. 13(*b*), the actual cleavage in $CuInSe_2$ takes place in zigzag {112} microcleavages, cutting across the tetrahedral bonds, as indicated by the dashed line *CD*. Thus, a macroscopic {110} 'cleavage' actually consists of {112} microcleavages.

The {101} plane has been previously reported to be a cleavage plane in natural crystals of the chalcopyrite mineral $CuFeS_2$ (Wolff & Broder, 1959; Berry, Mason & Dietrich, 1983) as well as in $CuInSe_2$. However, to the authors' knowledge there are no reports of such a cleavage plane in either the diamond or the zinc blende structures, where the corresponding cubic description of this plane would be {201}. Accordingly, the question is raised: why is the {101} plane a predominant cleavage plane in the chalcopyrite structure and, furthermore, why is it even more in evidence than the {112} plane in the $CuInSe_2$ crystals? Fig. 14 shows a view of a $CuInSe_2$ lattice, where the {101} planes are perpendicular to the paper. Shown also are the depth layers of the atoms below the {010} plane of the page, where the surface atoms are vertically above those in the fourth layer. Within the unit cell of size **a** x **a** x **2a**, where **a** is the length of the cell's smaller side, a {101} plane perpendicular to the paper has been marked by a broken line between the Se and the In atoms. Counting the number of bonds involved indicates that a cut along this plane has to break eight of the short tetrahedral bonds to separate the cell into two parts; six of these are Se—In bonds, while two are Se—Cu bonds. Since

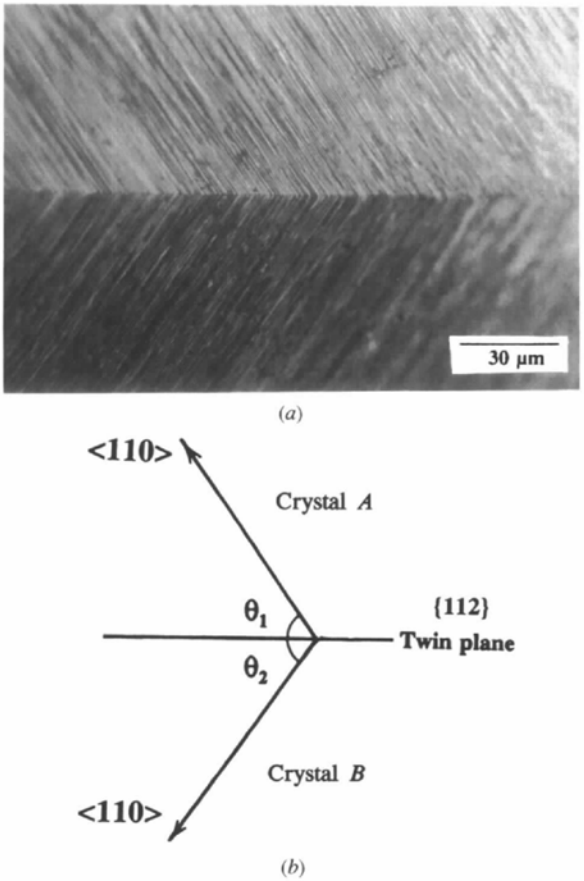

Fig. 9. Photomicrograph showing the {112} twinning plane boundary between two crystals having a {110} cleavage plane. The ridges in the photograph (*a*) point in the <110> direction in both crystals and make an equal angle of about 55° with the {112} twinning plane, as shown in the schematic (*b*).

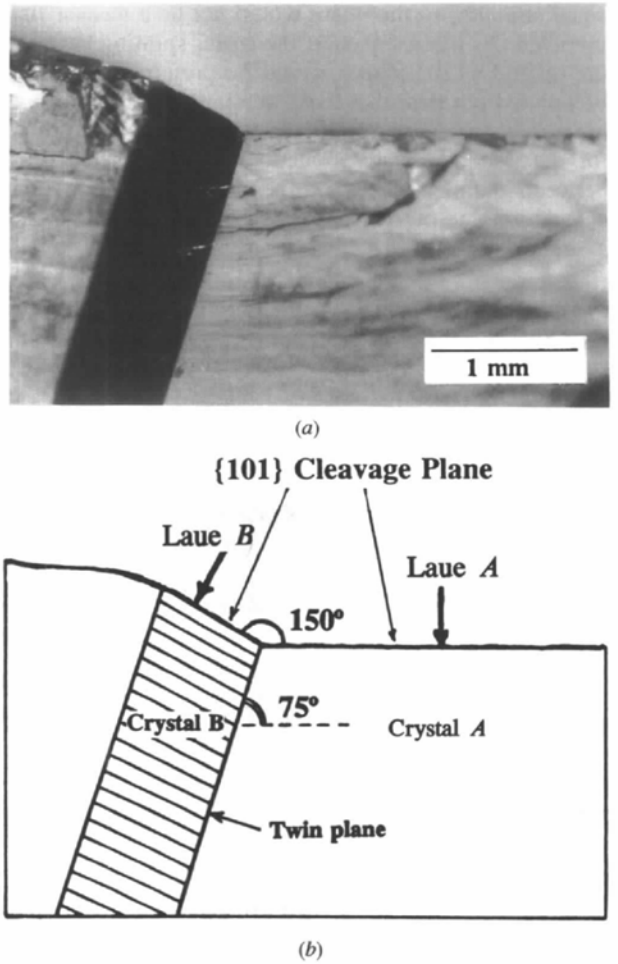

Fig. 10. (*a*) Photograph of a twinned $CuInSe_2$ sample cleaved in the {101} plane. (*b*) Schematic showing the twinned region in this sample and the position of the two Laue pictures of Fig. 11.

the Se—In bond is weaker (247 kJ mol^{-1} for a diatomic molecule) than the Se—Cu bond (293 kJ mol^{-1}), such a cut would require less effort per unit area than a parallel cut between the Se and Cu atoms, involving six Se—Cu bonds and two Se—In bonds. In comparison with the {112} plane, cleavage along the {101} plane with six Se—In and two Se—Cu bonds would also seem more favourable. While the {101} plane has a density of **total** bonds of $8/(5)^{1/2}$ per $\mathbf{a}^2$ and the {112} plane has the smaller value of $4/(3)^{1/2}$, the former plane has only 25% of the stronger Se—Cu bonds to break, but the latter plane has 50%. Taking this into account, this {101} cut involves breaking some 77%, that is to say $\frac{1}{4}[8/(5)^{1/2}]/\frac{1}{2}[4/(3)^{1/2}] = (3/5)^{1/2}$ or 0.77, less of the stronger bonds per $\mathbf{a}^2$ than a {112} cut. This argument, however, ignores the total energy required to break all the bonds, weak and strong, which would then favour {112} cleavage.

In the case of the zinc blende lattice, however, a corresponding {201} cut would also require the breaking of eight bonds per cell but here, the bonds would be of equal strength, so that there would not be a weaker link involved. As a consequence, the easier splitting between the neutral {110} planes would be preferred. It should be pointed out here that these qualitative considerations are purely speculative and in no way can they substitute for detailed quantitative calculations of least energies between parallel planes of the atoms involved. Such calculations lie outside the scope of this study.

Regarding the X-ray diffractograms, besides confirming the orientation and yielding the correct *d*-spacing for the different planes, the results also indicated that certain reflections, which are absent in polycrystalline samples, were present in the single crystal samples and these were the {224} reflection from the {112} cleavage plane, the {110} and {440} reflections from the {110} cleavage plane and the {303} and {404} reflections from the {101} plane. In the last two cleavage planes, two reflections were missing and these were the {330} from the {110} cleavage and the {202} from the {101} sample. It is possible that the intensities of these reflections were too weak to detect, particularly since the {202} reflection has been observed on samples, not presented in this study. In the case of silicon, certain reflections are expected to be missing because they are 'forbidden', since they have a zero geometrical scattering factor. However, unlike the diamond structure, where all the atoms are identical, the chalcopyrite structure has three different atom types with different atomic scattering factors (due to the different atomic numbers of 29, 49 and 34 for Cu, In and Se, respectively) and, therefore, weak reflections might be expected. As a result, the {110} reflection, forbidden in diamond, was detected as a weak line in these $CuInSe_2$ crystals.

The present observed twinning in the {112} plane in $CuInSe_2$ is the first reported clear identification of this orientation in a detailed study of bulk monocrystalline material. However, microtwins in this plane were

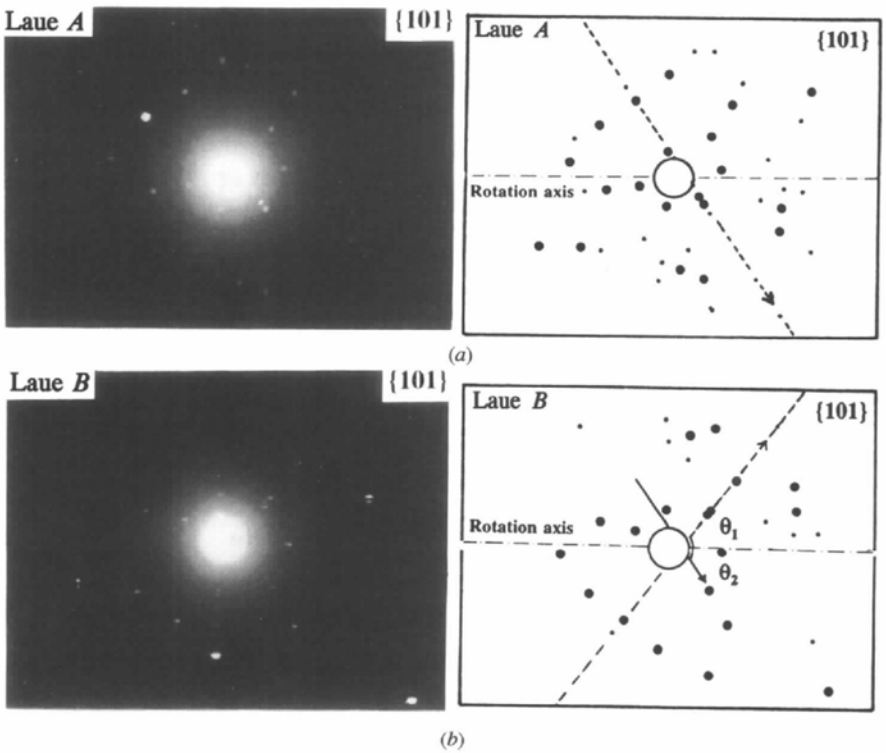

Fig. 11. X-ray Laue photographs on the twinned {101}-cleaved sample of Fig. 10. (*a*) Pattern of crystal *A* (Laue *A*); (*b*) pattern of the twinned crystal *B* (Laue *B*). The schematics show the coincidence of the spot pattern by a rotation of 180°, about an axis indicated by the horizontal chain line. The broken lines in (*a*) and (*b*) indicate the symmetry axis of each crystal. The angles θ_1 and θ_2 are equal.

found by Kiely, Pond, Kenshole & Rockett (1991) in polycrystalline material and by Xiao, Yang & Rockett (1994) in the related compound $CuIn_3Se_5$. The result is not different from the case of silicon (Salkovitz & von Batchelder, 1952), GaAs or CdTe (Lorenz, 1962), where twinning occurs along the equivalent {111} plane in these materials. This comes back to the face-centred-cubic lattice, on which the diamond, zinc blende and the chalcopyrite structures are based, where twinning also occurs along the {111} plane.

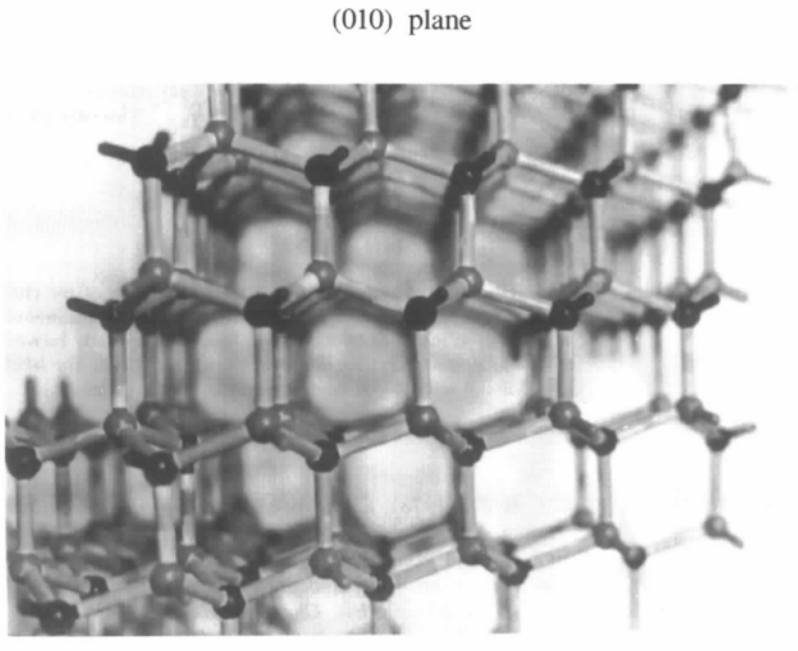

(*a*)

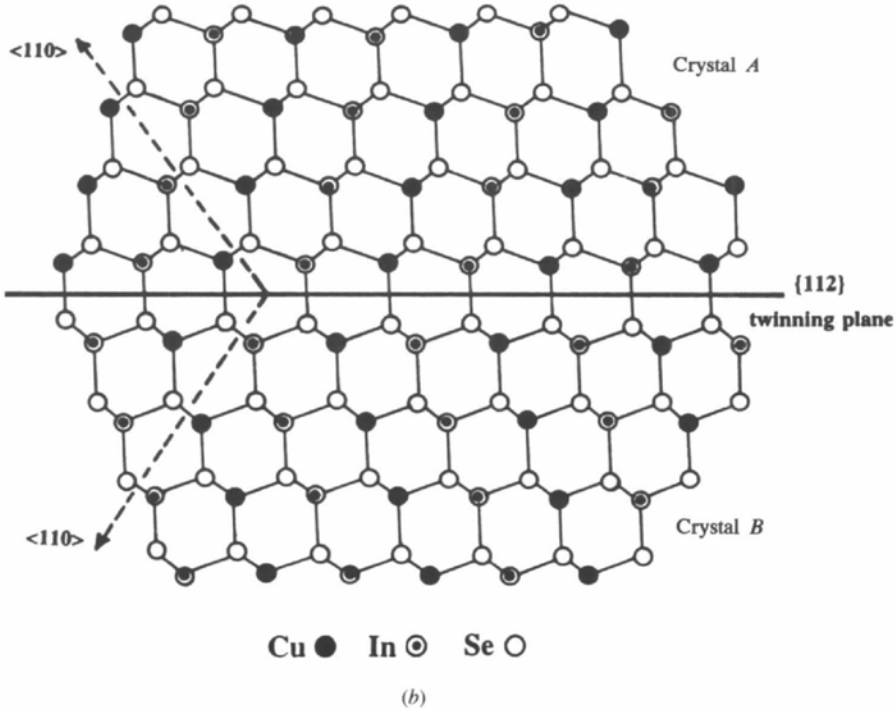

(*b*)

Fig. 12. (*a*) Photograph of a 'ball' and 'stick' crystal model and (*b*) schematic showing twinning in the chalcopyrite structure, where the {110} plane is the plane of the page. The schematic shows the {112} twinning plane perpendicular to the page and makes equal angles (54.74°) with the indicated <110> directions (broken arrows) on the two crystals.

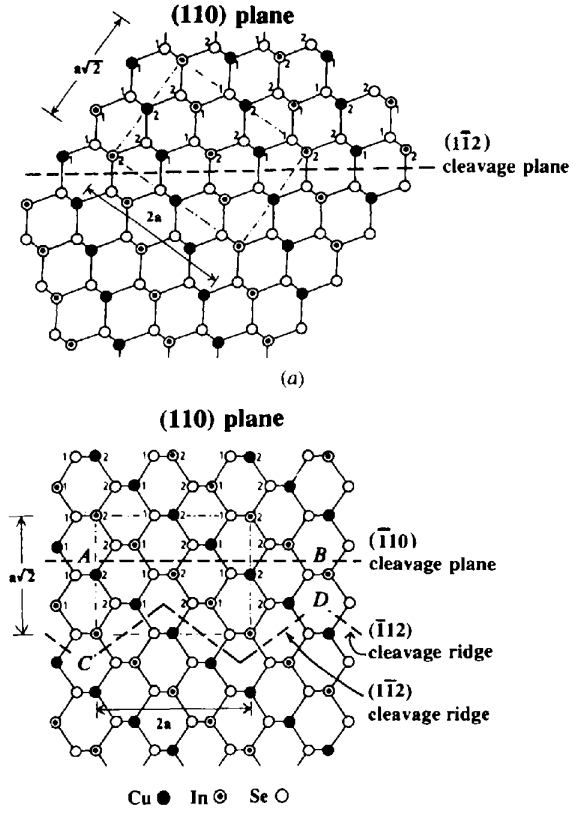

Fig. 13. Schematic of atomic layers of the (110) plane of the chalcopyrite structure, viewed with the (112) plane (*a*) horizontal and (*b*) rotated by about 35°. Cleavage planes normal to the page are indicated by the broken lines for (*a*) a (112) cleavage and (*b*) two possible (110) cleavages indicated as *AB* and *CD*. The chain line represents the unit cell in each plane. The labels 1 and 2 refer to consecutive depth layers of the atoms.

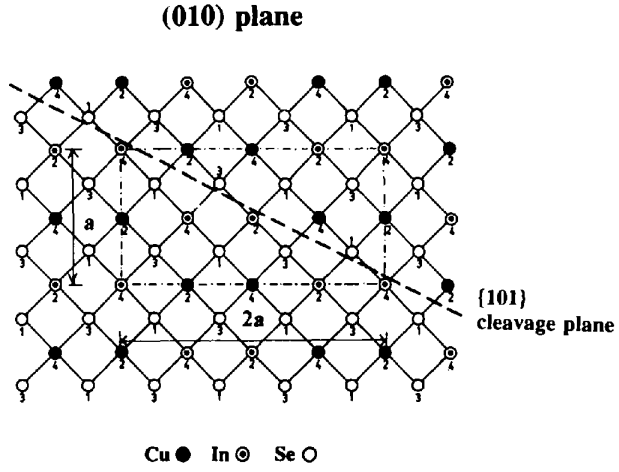

Fig. 14. Schematic of atomic layers of the (010) plane of the chalcopyrite structure showing a possible {101} cleavage plane, normal to the page, as indicated by the broken line, predominantly between In and Se atoms. The chain line represents the unit cell. The labels 1, 2, 3 and 4 refer to consecutive depth layers of the atoms.

The authors wish to acknowledge support of this work by the Natural Sciences and Engineering Research Council of Canada under their Strategic Grants Program.

References

Abrahams, M. S. & Ekstrom, L. (1960). *Acta Metall.* **8**, 654–662.

Bean, K. E. & Gleim, P. S. (1969). *Proc. IEEE*, **57**, 1469–1476.

Berry, L. G., Mason, B. H. & Dietrich, R. V. (1983). *Mineralogy*, pp. 261–262. New York: W. H. Freeman & Co.

Cullity, B. D. (1978). *Elements of X-ray Diffraction*, p. 502. Reading, Massachusetts: Addison Wesley Publishing Co.

Ghandi, S. K. (1983). *VLSI Fabrication Principles*, pp. 13–14. New York: John Wiley and Sons Inc.

Holt, D. B. (1964). *J. Phys. Chem. Solids*, **25**, 1385–1395.

Iwanaga, H., Tomizuka, A. & Shoji, T. (1991). *J. Mater. Sci. Lett.* **10**, 975–977.

Kiely, C. J., Pond, R. C., Kenshole, G. & Rockett, A. (1991). *Philos. Mag. A*, **63**, 1249–1273.

Lorenz, M. R. (1962). *J. Appl. Phys.* **33**, 3304–3306.

Massopust, T. P., Ireland, P. J., Kazmerski, L. L. & Bachmann, K. J. (1984). *J. Vac. Sci. Technol. A*, **2**, 1123–1128.

Pfister, H. (1955). *Z. Naturforsch. Teil A*, **10**, 79.

Salkovitz, E. I. & von Batchelder, F. W. (1952). *J. Met.* **4**, 165.

Shahidi, A. V., Shih, I., Araki, T. & Champness, C. H. (1985). *J. Electron. Mater.* **14**, 297–310.

Shukri, Z. A., Champness, C. H. & Shih, I. (1993). *J. Cryst. Growth*, **129**, 107–110.

Wolff, G. A. & Broder, J. D. (1959). *Acta Cryst.* **12**, 313–323.

Xiao, H. Z., Yang, L.-C. & Rockett, A. (1994). *J. Appl. Phys.* **76**, 1503–1510.

Yip, L. S., Shih, I. & Champness, C. H. (1993). *J. Cryst. Growth*, **129**, 102–106.

Yip, L. S., Weng, W. S., Li, L., Shih, I. & Champness, C. H. (1991). *Proceedings of the 10th PVSEC International Conference*, 921–923. Dordrecht: Kluwer Academic Publishers.